SOVIET PHYSICS

# USPEKHI

*A Translation of Uspekhi Fizicheskikh Nauk*



SOVIET PHYSICS USPEKHI (Russian Vol. 97, Nos. 3 and 4) SEPTEMBER-OCTOBER 1969

535

## *THE RING GAS LASER*

V. E. PRIVALOV and S. A. FRIDRIKHOV

Leningrad Polytechnic Institute

Usp. Fiz. Nauk 97, 377–402 (March, 1969)

IN the first lasers, use was made of a Fabry-Perot resonator (flat mirrors). To decrease the diffraction losses, the flat mirrors were subsequently replaced by spherical ones. The field structure in a flat-mirror resonator containing lenses is similar to the field structure in a resonator with spherical mirrors in a certain region, and similar to the field structure of a ring resonator in the entire region. From this point of view, a ring resonator can be regarded as the most general type of resonator.

A laser with a ring resonator can be used to measure angular rotation velocities with high accuracy, and it is superior to all the hitherto known devices.[1,2] This is one of the reasons why great interest attaches to the use of a laser of this type for navigational purposes.[3-5] The high monochromaticity and continuity of the operating conditions, which are needed for this case, govern the choice of the active medium used in a laser intended for such measurements. The initial investigations in this direction hardly dealt with the processes in the active medium. The discharge tube was considered in these investigations as some sort of "black box." As new effects became known, the investigators started to pay more and more attention to the features of the behavior of the active medium in a ring resonator. The study of the physical processes that determine the main properties of the ring laser becomes more and more timely. It is also to be expected that new theoretical and experimental investigations will make it possible not only to increase the possibility of measuring the angular rotation velocity, but also to expand the scope of the applications of ring lasers with various active media. The purpose of the present view is to consider the main properties of a ring resonator and of the gaseous active medium placed in this resonator, and to systematize the published data on this subject.

## 1. FUNDAMENTAL EQUATIONS FOR THE RING RESONATOR

From Maxwell's equations, which describe the electromagnetic field in free space, we can obtain the wave equation for the electric field $\mathbf{E}$[6]

$$\Box \mathbf{E} = 0, \tag{1.1}$$

where $\Box$ is the d'Alambert operator. The Green's function for this equation is $r^{-1}\exp(-i\mathbf{k}\cdot\mathbf{r})$. In the case of two reflecting surfaces, the situation becomes somewhat more complicated, and the solution of (1.1) is written in the form[7]

$$E_1 = \frac{ik}{4\pi}\int_S \frac{1+\cos\theta}{r}\exp(-ikr)\,E_2\,dS, \tag{1.2}$$

where $E_m$ is the field of the m-th mirror (m = 1, 2), r is the radius vector, S is the surface of the mirror with $E_2$, and $\theta$ is the angle between $\mathbf{r}$ and the normal to the mirror at the initial point of $\mathbf{r}$ (Fig. 1).

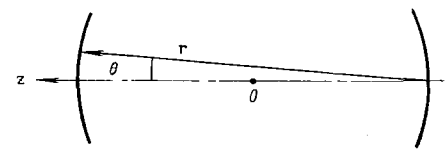


FIG. 1. Linear resonator with two spherical mirrors.

By analyzing the Huyghens principle in the Fresnel-Kirchhoff form in the scalar form (1.2), we can obtain[8] the fundamental relations for an optical resonator with two mirrors (we shall call it a linear resonator).

Many fundamental papers have been published by now, considering the linear resonator from various points of view (see, for example,[9-14]). The most convenient to analyze is the confocal resonator, which is frequently employed in practice, owing to its low diffraction loss.

The frequency spectrum of this resonator is determined by the equation[10]

$$\nu = \frac{c}{2L}\left[q + \frac{1}{2}(m+n+1)\right], \tag{1.3}$$

where L is the radius of curvature of the mirrors, equal to the distance between them, m, n, and q are indices characterizing the oscillation mode (q—longitudinal modes, m and n—transverse modes).

The field inside the resonator is given by

$$E = E_0 \left(\frac{2}{1+\xi^2}\right) \frac{\Gamma\left(\frac{m}{2}+1\right)\Gamma\left(\frac{n}{2}+1\right)}{\Gamma(m+1)\,\Gamma(n+1)} H_m\left(X\sqrt{\frac{2}{1+\xi^2}}\right) H_n\left(Y\sqrt{\frac{2}{1+\xi^2}}\right) \times \exp\left[-\frac{k(x^2+y^2)}{L(1+\xi^2)}\right] \exp\left(-i\left\{k\left[\frac{L}{2}(1+\xi)+\frac{\xi(x^2+y^2)}{(1+\xi^2)L}\right] - (1+m+n)\left(\frac{\pi}{2}-\varphi\right)\right\}\right), \quad (1.4)$$

where

$$\xi = \frac{2z}{L}, \quad X = \frac{x\sqrt{c}}{a}, \quad Y = \frac{y\sqrt{c}}{a}, \quad c = \frac{2\pi a^2}{L\lambda}, \quad \varphi = \operatorname{arctg}\frac{1-\xi}{1+\xi},$$

$H_m$ and $H_n$ are Hermitian polynomials of orders m and n, respectively, and $\Gamma$ is the Gamma function. The distribution of the $TEM_{00q}$ mode field intensity in the (x, y) plane has the form shown in Fig. 2.

The wave front at each point z (origin at the focus of the mirror) has a curvature radius

$$R(z) = \frac{L^2+4z^2}{4z}. \quad (1.5)$$

For the fundamental mode, the radius of the beam (at which the field is decreased by a factor e compared with the value on the resonator axis) is:

$$w(z) = \sqrt{\frac{L}{k}\left[1+\left(\frac{2z}{L}\right)^2\right]}. \quad (1.6)$$

Any confocal resonator with mirrors 1 and 2 (Fig. 3) can be represented by an equivalent resonator.

Indeed, it follows from (1.5) that if the front curvature at the point $z_3$ is 1/b, then there exist also other points where the curvature has the same value. Let the coordinates of these points be $z = \pm d/2$; then they are separated pairwise by a distance $d = b \pm \sqrt{b^2 - L^2}$. It is seen from Fig. 3 that a confocal resonator with mirrors 1 and 2 separated by a distance L is equivalent to three resonators, the mirrors of which have curvatures 1/b and are separated from each other by distances $d_1$, $d_2$, and b.

Thus, the analysis of a resonator of any kind can be carried out by choosing a confocal resonator as the basis. In particular, the spectrum of a linear resonator with arbitrary parameters can be written in general form[13] as

$$\nu = \frac{c}{2L}\left(q + \frac{m+n+1}{\pi}\arccos\sqrt{g_1 g_2}\right), \quad (1.7)$$

where $g_i = 1 - (L/R_i)$ (i = 1, 2, $R_i$ is the radius of curvature of the mirrors, and L is the distance between the mirrors).

The situation is somewhat different in the case of a resonator having two flat mirrors. It was investigated earlier (with external radiation incident on a Fabry-Perot etalon) by very simple methods (the summation method, the edge-value method[7]), and later by other methods,[8,11,14,15] which are convenient, in principle, for all resonators.

The spectrum of such a resonator is

$$\nu = \frac{c}{2L}\left(q + \frac{\pi m^2}{|\beta(1+i)+M|^2}\right), \quad (1.8)$$

where $M = 2\sqrt{2\pi N}$, $\beta$ is a parameter determined by the reflection coefficient, $N = a^2/\lambda L$ is the Fresnel number, a is the diameter of the mirror, and m = 1, 2, 3....

In some cases (for example, to produce a field structure equivalent to a confocal resonator in a resonator with flat mirrors),[16] lenses are placed inside the resonator. In this case, the characteristics of the field in the resonator, naturally, change. It turns out here that any inhomogeneity inside the resonator can be made equivalent to a lens. In the analysis of such a resonator (Fig. 4), one can seek the field, in accordance with the Huyghens principle, in the form of a product, each factor of which is represented by expression (1.2) written out for all the remaining objects of the resonator.[17] It is required here that: 1) the fields on the mirrors be expressed in similar fashion; 2) that the variables be separable; 3) that the field be written in analogy with (1.4).

On the basis of these three postulates, it is possible to obtain the dimensions of the field spots for the resonator shown in Fig. 4:

$$\mu_{i0} = k\,|\rho_{\mu ii}|\sqrt{\frac{\rho_{\mu 1N}^2}{4\rho_{\mu 11}\rho_{\mu NN}} - 1}, \quad (1.8')$$

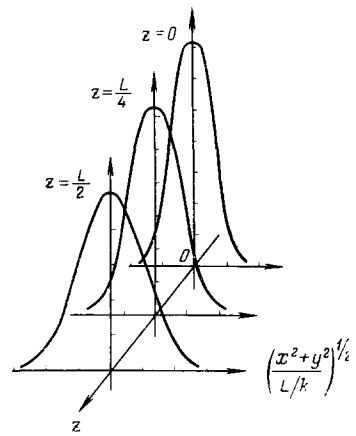


FIG. 2. Distribution of the $TEM_{00q}$ mode field intensity in the cross section of a confocal linear resonator. L—resonator length.

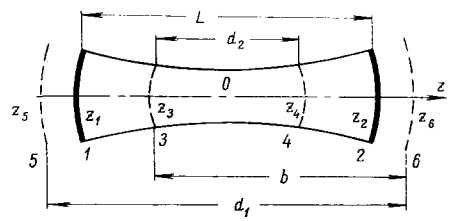


FIG. 3. Field distribution in the longitudinal cross section of a confocal linear resonator. The dashed lines showed the equal-phase surfaces of the resonator.

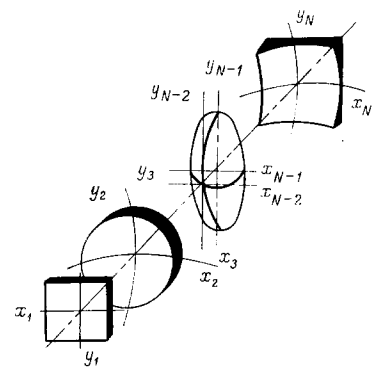


FIG. 4. Linear resonator with lenses.

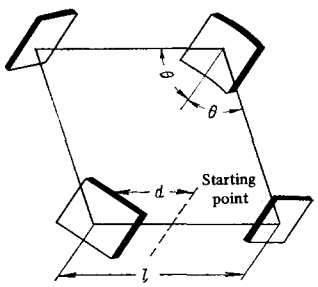


FIG. 5. Ring resonator with one spherical and three flat mirrors [17].

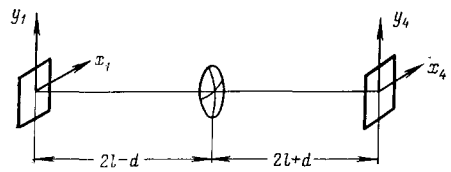


FIG. 6. Linear resonator with elliptical lens; this resonator is equivalent to a ring resonator [17].

where $\rho_{\mu ii}$ are the coefficients of the optical distances, and the frequency spectrum is given by the formula

$$\nu = \frac{c}{2\rho_0}\left[\gamma q + \left(n + \frac{1}{2}\right)\frac{\alpha_x}{\pi} + \varepsilon + \left(m + \frac{1}{2}\right)\frac{\alpha_y}{\pi}\right], \qquad (1.9)$$

and

$$\cos\alpha_\mu = \sqrt{\frac{4\rho_{\mu 11}\rho_{\mu NN}}{\rho^2_{\mu 1N}}} \quad \left(\mu = x,\ y,\ \varepsilon = 0,\ \frac{1}{2}\right).$$

For a linear resonator, $\gamma = 1$ and $\epsilon = 0$.

This problem can be solved by direct integration of the fundamental equations, which leads to the same result.[18-21] An analysis presented in [17-20] is a generalization of the theory of a linear (and not only a linear) resonator. A resonator with an inhomogeneity is equivalent to a ring resonator.[18-21] Therefore the schemes of Figs. 5 and 6 are equivalent. In Fig. 6, an elliptical lens, which projects the different focal distances of a spherical mirror of Fig. 5 on the vertical and horizontal planes ($f_x = R\cos\theta/2$, $f_y = R\sec\theta/2$), is placed in the resonator.

The coefficients of the optical distances for such a ring resonator are given by the following formulas[17]

$$\rho_0 = 4l,$$
$$\rho_{\mu 11} = \rho_{\mu 44} = \frac{1 - \frac{2l}{f_\mu}}{2f_\mu\left[1 - \left(1 - \frac{2l}{f_\mu}\right)^2\right]},$$
$$\rho_{\mu 14} = \frac{1}{f_\mu\left[1 - \left(1 - \frac{2l}{f_\mu}\right)^2\right]}.$$

Knowing these coefficients, we can write the main parameters of the ring resonator. The frequency spectrum, in particular, is given by:

$$\nu = \frac{c}{4l}\left[q + \frac{\alpha_x}{\pi}\left(n + \frac{1}{2}\right) + \frac{\alpha_y}{\pi}\left(m + \frac{1}{2}\right)\right], \qquad (1.10)$$
$$\cos\alpha_\mu = 1 - \frac{2l}{f_\mu}.$$

Such a transformation of (1.9) is possible because in the case of a ring resonator $\gamma = 2$, and $\epsilon \neq 0$ only if the number of the mirrors and n are both simultaneously odd.

The frequency spectrum of a triangular ring resonator is written in the form[22]

$$\nu = \begin{cases} \frac{c}{L}\left[q + \frac{\alpha_x}{\pi}(n+1) + \frac{\alpha_y}{\pi}(m+1)\right], & n - \text{even}, \\ \frac{c}{L}\left[q + \frac{1}{2} + \frac{\alpha_x}{\pi}(n+1) + \frac{\alpha_y}{\pi}(m+1)\right], & n - \text{odd}, \end{cases} \qquad (1.11)$$

where L is the perimeter of the triangle. The spectrum of the ring resonator can be obtained also by geometrical-optics methods.[23,24]

On concluding this section, we point out one more possible generalization in the analysis of optical resonators. Just like the stability diagram[17] of a resonator with an inhomogeneity, plotted in coordinates $2\rho_{\mu NN}/\rho_{\mu 1N}$ (ordinate axis) and $2\rho_{\mu 11}/\rho_{\mu 14}$, can be used in the case of an arbitrary resonator (for a linear resonator it is given in [9]), the plot of $1/R_z$ (ordinates) vs. $z/kw^2$ can be used to describe the properties of the field at any point of the resonator.[17] By eliminating z from (1.5) and (1.6) we obtain

$$\left(\frac{2}{kw^2} - \frac{1}{L}\right)^2 + \frac{1}{R_z^2} = \frac{1}{L^2}. \qquad (1.12)$$

Equation (1.12) corresponds to a family of circles (Fig. 7). Each confocal resonator with perimeter $L_i$ has its own circle. The points on the circle correspond to a displacement inside the resonator. With increasing L, the circles decrease.

By eliminating L from (1.5) and (1.6) we obtain an equation of another family of circles (dashed line in Fig. 7):

$$\left(\frac{2}{kw^2}\right)^2 + \left(\frac{1}{R_z} - \frac{1}{2z}\right)^2 = \left(\frac{1}{2z}\right)^2.$$

A displacement inside the resonator corresponds here to a transition from one circle to another. For a ring

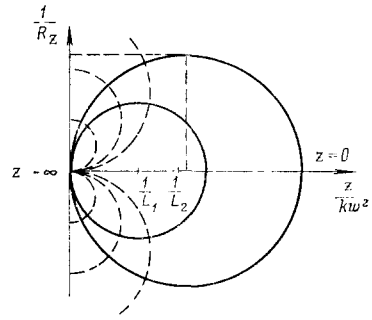


FIG. 7. Diagram describing the distribution of the field in a confocal resonator [17].

resonator (four flat mirrors) with a lens, we obtain the diagram shown in Fig. 8. In the case of a triangular resonator[22] we obtain a similar diagram, the diagrams for the vertical and horizontal planes being different.

## 2. ROTATION OF RING RESONATOR

Let us consider a square ring resonator, in which the light beam follows the perimeter of a square (Fig. 9). In the case of a stationary resonator, the light has a frequency $\nu$ in the system A (and at any other point of the resonator). In the case of rotation in the direction

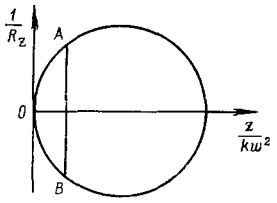


FIG. 8. Diagram characterizing the field distribution in a ring resonator with four flat mirrors and a lens [17].

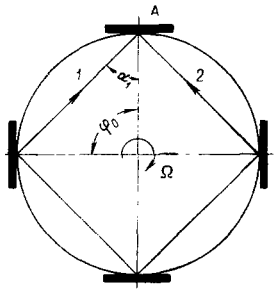


FIG. 9. Quadratic ring resonator. 1—angle of incidence of beam on the mirror. $\alpha_1$—angle of beam incidence on mirror, $\varphi_0$—angle between mirrors of laser at rest, $\Omega$—angular velocity of ring resonator.

indicated by the arrow, with frequency $\Omega$ in the reference system of the mirror A, the frequency of the light propagating in the direction 1 becomes different. The Lorentz transformations for the wave vector **k** yield[6]

$$k_4' = \frac{k_4 + i\beta k_1}{\sqrt{1-\beta^2}},$$
$$k_4 = 2\pi i \frac{\nu}{c},$$
$$k_1 = \frac{2\pi\nu}{c}\cos\alpha_1, \qquad (2.1)$$

where $k_i$ (i = 1, 2, 3, 4) is the component of the wave vector **k** in the fixed coordinate system, $k_i'$ are the components of the wave vector in the coordinate system moving with velocity v relative to the fixed system, c is the velocity of light, $\beta = v/c$, and $\alpha_i$ (i = 1, 2, 3) is the angle of incidence of the beam on the mirror.

This means that in the system of the mirror A there occurs a shift of the frequency of the light (Doppler effect of the first order) compared with the stationary case, by an amount

$$\Delta_1\nu = \beta\nu\cos\alpha_1 \quad (\beta \ll 1). \qquad (2.2)$$

A similar reasoning can be used also for beam 2. In this case a shift of the frequency in the opposite direction will take place, by an amount $\Delta\nu_2 = |\Delta\nu_1|$. Thus, when the ring resonator rotates, two frequencies appear at the output of the mirror A, differing by an amount

$$\Delta\nu = 2\beta\nu\cos\alpha. \qquad (2.3)$$

From this general formula for the frequency splitting in the nonrelativistic case we can obtain similar relations for a resonator of any geometry.

In particular, for a quadratic resonator

$$\Delta\nu = \frac{\Omega\nu l}{c}, \qquad (2.4)$$

where $l$ is the side of the square.

This result can be obtained in various manners. Since analysis of each of them yields certain information concerning the ring resonator, we shall stop to discuss one more method of deriving (2.4).[25,26] When $\Omega = 0$, each side of the square belongs to a central angle $\varphi_0 = \pi/2$ (see Fig. 9). In the case of rotation, this angle increases or decreases, depending on the direction of the rotation:

$$\varphi_\pm = \frac{\pi}{2} \pm \frac{\Omega\tau_\pm}{4},$$

where $\tau_\pm$ is the time in which the light returns to the initial point. The travel time difference between the two rays is

$$\Delta\tau = \frac{8\Omega R^2}{c^2},$$

where R is the radius of rotation of the mirrors.

The frequency variation due to the Doppler effect can be written in the form[7]

$$\Delta\nu_\pm = \nu\frac{\Delta t}{t}, \qquad (2.5)$$

where t is the time of one cycle.

In our case $t = \tau$ and $\Delta t = \Delta\tau/2$. Therefore

$$\Delta\nu_+ = \nu\frac{\Delta\tau}{2\left(\tau_0 - \frac{\Delta\tau}{2}\right)} = \frac{1}{2}\frac{\beta\nu l^2}{\sqrt{2}R^2 + \frac{1}{2}\beta l^2},$$
$$|\Delta\nu_+| = |\Delta\nu_-| = \frac{1}{2}|\Delta\nu|;$$

when $\beta \ll 1$ we have

$$\Delta\nu = \frac{\Omega\nu l}{c},$$

as in (2.4).

In experiments by Sagnac[25,26] with an interferometer of a somewhat different construction (Fig. 10), a semitransparent mirror was placed in a position normal to the positions of the other mirrors along the circles. In analogy with (2.1), in this case the Lorentz transformation for the wave vector of beam 2 reflected from the mirror yields

$$\bar{k}_4' = \frac{k_4 - i\beta k_1}{\sqrt{1-\beta^2}}. \qquad (2.6)$$

For beam 1, which passes through mirror A and completes the resonator in the counterclockwise direction, the frequency in the system of the moving mirror A is transformed in accordance with formula (2.1), i.e., in the case of a moving mirror, the frequency of the incident beam differs from that of the reflected one. This difference is determined from the difference between $k_4'$ and $\bar{k}_4'$:

$$\Delta\nu = 2\beta\nu\cos\alpha \quad (\beta \ll 1). \qquad (2.7)$$

It is easy to show that the change of frequency occurring upon reflection from the remaining mirrors, in the coordinate systems of these mirrors, does not result in a

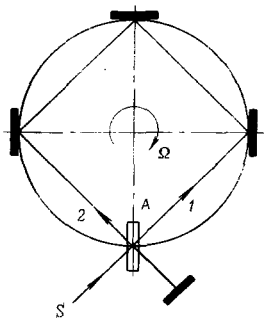


FIG. 10. The Sagnac interferometer [25, 26].

change of the frequency in the system of the mirror A. The difference between the frequencies of rays 1 and 2, which enter into the receiver after completing the circuit, is determined only by formula (2.7), which coincides with the previously given formula (2.3).

Let us consider now the same situation from several different points of view. When the resonator rotates, the length of the optical path changes, and with it the natural frequencies of the resonator:[27]

$$\frac{\Delta\nu}{\nu} = \frac{\Delta L}{L}. \tag{2.8}$$

On the basis of this, a formula was obtained for [28] for the frequency shift of a (square) ring resonator

$$\Delta\nu = \frac{\Omega l}{\lambda}\cos\gamma, \tag{2.9}$$

where $\gamma$ is the angle between the vector $\Omega$ and the normal to the plane of the beam. This approach is used by the authors of [1], who were among the first to investigate experimentally the frequency splitting in an He-Ne laser with a ring resonator. The same approach was used in [29]. It is obvious that it contains nothing new compared with the ideas discussed in the analysis of Fig. 9. The analysis of a resonator in the form of a continuous ring admits of another interpretation.[30]

We can consider the interference of waves moving opposite to each other in the gravitational field of a rotating ring resonator, and obtain a formula for the phase shift.[31] From this point of view, it is convenient to analyze the frequency spectrum of a rotating resonator. The analysis is carried out in the following manner.[32] The field of the resonator, in accordance with [33], is sought in the form

$$E = \sum_{\alpha} E_{\alpha} \int EE_{\alpha}^{*}\, dv + \sum_{\beta} F_{\beta} \int EF_{\beta}^{*}\, dv, \tag{2.10}$$

where F is the electromagnetic field tensor. Substituting (2.10) into Maxwell's equations and taking into account the fact that in a rotating coordinate system the induction D is replaced by

$$\mathbf{D}_e = k_e\mathbf{E} - \frac{1}{c}\left[\frac{\Omega\mathbf{x}\mathbf{r}}{c}\,\mathbf{H}\right],$$

(here $k_e$ is the dielectric constant, x is the coordinate, r is the vector characterizing the position of the rotation axis in the plane of the ray,* we obtain for a plane wave†

$$\nu_a = \nu_a^0\left\{1 + \tfrac{1}{2}(k_e k_m c^2)^{-\frac{1}{2}}\Omega\int[\mathbf{r}x([\mathbf{E}_a^{*}\mathbf{H}_a] + [\mathbf{E}_a\mathbf{H}_a^{*}])]\, dv\right\}\cos\gamma,$$

where $\nu_a$ are the natural frequencies of the ring resonator. Since there are two such waves, the frequency difference between them is

$$\Delta\nu = \nu_a(k_e k_m c^2)^{-\frac{1}{2}}\Omega\int\mathbf{r}x([\mathbf{E}_a\mathbf{H}_a^{*}] + [\mathbf{E}_a^{*}\mathbf{H}_a])\cos\gamma\, dv. \tag{2.11}$$

Expression (2.11) is the most general among the previously obtained equations for the frequency splitting following rotation of the ring resonator. In the case of a quadratic resonator in vacuum, we obtain from (2.11) the already familiar formula

$$\Delta\nu = \frac{\Omega l v}{c}\cos\gamma.$$

The presence of an active medium in a quadratic resonator leads to the expression

$$\Delta\nu = \frac{\Omega v l}{c}\left\{1 - \frac{a}{4l}[1 - (k_e k_m)]^{-\frac{1}{2}}\right\}\cos\gamma, \tag{2.12}$$

where a is the length of the active medium.

In addition to the active medium, there can be situated in a ring resonator additional elements, for example a moving medium (the purpose of the latter will become clear in Ch. 6). This leads to the appearance of new terms in the expression for the frequency splitting in the ring resonator. For a moving medium (with refractive index $n_0$) of length d in a ring resonator, this expression takes the form[34]

$$\Delta\nu = \nu\frac{4\frac{\Omega S}{c} - 2d\left(n_0 - 1 - \nu n_0\frac{dn_0}{d\nu}\right)\frac{\mathbf{V}\mathbf{v}}{c}}{L - d(n_0 - 1) + \nu d\frac{dn_0}{d\nu} + a\nu\frac{dn_a}{d\nu}}, \tag{2.13}$$

where v is the velocity of the medium with the refractive index $n_0$, S is the area of the annular resonator, V is a unit vector in the direction of light propagation, and $n_a$ is the refractive index of an active medium of length a.

Expression (2.13) was obtained by considering the tensor of the dielectric constant of the medium in a rotating resonator. This method can be used in a particular case to derive also expression (2.12).

## 3. FUNDAMENTALS OF THE THEORY OF A RING RESONATOR WITH A GASEOUS ACTIVE MEDIUM

The behavior of the active medium in a laser is best characterized by the macroscopic polarizability of the medium P. The general method of analyzing a gas laser[35] is applicable also in the case of a ring gas laser (for example, [36]). Maxwell's equations with the boundary conditions customary for an absorbing medium make it possible to write for an electric field E the following wave equation:

$$[\nabla[\nabla, \mathbf{E}]] + \mu\sigma\frac{\partial\mathbf{E}}{\partial t} + \mu\varepsilon\frac{\partial^2\mathbf{E}}{\partial t^2} + \mu\frac{\partial^2\mathbf{P}}{\partial t^2} = 0, \tag{3.1}$$

where $\mu$ is the magnetic permeability, $\epsilon$ is the dielectric constant, and $\sigma$ the conductivity of the medium.

Confining ourselves to the fundamental mode, neglecting the dependence on x and y, and assuming the Q factor of the resonator at the frequency $\nu_n$ to be

$$Q_n = \frac{\varepsilon\nu_n}{\sigma}, \tag{3.2}$$

we can write (3.1) for a plane-polarized wave in the following manner:

$$\frac{\partial^2 E}{\partial z^2} - \varepsilon\mu\frac{\nu_n}{Q_n}\frac{\partial E}{\partial t} - \varepsilon\mu\frac{\partial^2 E}{\partial t^2} = -\mu\nu^2 P. \tag{3.3}$$

The solution of (3.3) for a ring laser is sought in the form of two waves traveling opposite to each other*

$$E(z, t) = \sum_{n}[A_n(t)U_n(z) + \tilde{A}_n(t)V_n(z)], \tag{3.4}$$

where

$$U_n(z) = \sin k_n z,$$

*The magnetic induction B is transformed analogously.

†$[\mathbf{E}_{\alpha}^{*}\mathbf{H}_{\alpha}] \equiv \mathbf{E}_{\alpha}^{*} \times \mathbf{H}_{\alpha}$.

*The expansion is in terms of the natural frequencies of the resonator.

$$V_n(z) = \cos k_n z,$$
$$k_n = \frac{2\pi n}{L},$$

and L is the perimeter of the resonator.

Separation of the variables leads to the following relations:

$$\left(\frac{d^2}{dz^2} + \varepsilon\mu\Omega_n^2\right)\begin{pmatrix} U_n(z) \\ V_n(z)\end{pmatrix} = 0, \tag{3.5}$$

$$\left(\frac{d^2}{dt^2} + \frac{\nu}{Q}\frac{d}{dt} + \Omega_n^2\right)\begin{pmatrix} A_n(t) \\ \tilde{A}_n(t)\end{pmatrix} = \frac{\nu^2}{\varepsilon}\begin{pmatrix} P_n(t) \\ \tilde{P}_n(t)\end{pmatrix}, \tag{3.6}$$

where $P_n$ are the corresponding Fourier transforms of the polarizability.

From (3.6) we obtain self-consistent equations for the determination of the amplitudes, frequencies, and phases of both traveling waves. The number of equations in the case of a ring laser, naturally, is twice as large than in the case of a linear laser.[35] This is followed by analysis of the polarizability of the medium, knowledge of which is essential for the solution of the self-consistent equations. The polarizability is determined by the density-matrix method. In the first perturbation-theory approximation, the threshold conditions are obtained from the equations

$$\ddot{E}_i + \frac{1}{2}\frac{\nu}{Q}\dot{E}_i = \frac{1}{2}\frac{\nu}{\varepsilon}\sqrt{\pi}\,AE_i\exp(-\xi^2), \tag{3.7}$$

$$\nu_i = \Omega_i - \frac{\nu}{\varepsilon}AF(\xi), \tag{3.8}$$

where

$$F(\xi) = \exp(-\xi^2)\int_0^{\xi_i}\exp(x^2)\,dx,$$

$$A = \frac{(p)^2\bar{N}(t)}{\hbar ku}, \quad \xi = \frac{\nu_i - \nu}{ku};$$

p is the magnetic element of the electric dipole moment, $2(\ln 2)^{1/2}ku$ is the width of the Doppler contour, N(t) is the average density of the excited states, and u is the most probable velocity of the atom.

Expressions (3.7) and (3.8) are the result of an analysis of the following model: there are two standing waves; on changing over from the results obtained for a linear laser,[3,5] one traveling wave of each is cut off and we are left with two waves traveling opposite to each other and having different frequencies (3.8). This is precisely the situation realized in a rotating ring laser.

In the second perturbation-theory approximation, two dips appear on the velocity-distribution curve, and have different depths:

$$\Delta\rho(v_i t) = \bar{N}(t)W(v)\left\{1 - 2I_1\left[1 + 2\left(\frac{v - \nu_1 - ku}{\Delta\omega_n}\right)^2\right]^{-1} - 2I_2\left[1 + 2\left(\frac{v - \nu_1 - \Delta\Omega + ku}{\Delta\omega_n}\right)^2\right]^{-1}\right\},$$

where $I_i$ is the radiation intensity, $\Delta\rho$ the population inversion, and W the equilibrium atom-velocity distribution.

Further, in the third order of perturbation theory, we obtain the generation conditions. In place of $\exp(-\xi^2)$ there appears in (3.7) the factor

$$\frac{z_i(\xi)}{z_i(0)} = I_1\exp(-\xi_1^2) - I_2\exp(-\xi_1^2)L(\xi),$$

where

$$z_i(\xi) = \sqrt{\pi}\exp(-\xi^2) - 2\eta[1 - 2\xi F(\xi)] + \ldots,$$
$$\eta = \frac{\gamma_{ab}}{ku} = \frac{1}{2}\frac{\Delta\omega_n}{ku}, \quad L(\xi) = \left[1 + \left(\frac{\xi}{\eta}\right)^2\right]^{-1};$$

$\gamma_{ab}$ is the natural line width.

An analysis of the stability of the opposing-wave regime makes it possible to show[36] that the stability is minimal in the case when the frequencies of the opposing waves are equidistant from the center of the Doppler contour. The point is that in this situation interaction of the two waves proceeds via one group of atoms, i.e., the coupling is maximal. The process of a second isotope (for example $Ne_{20}$ and $Ne_{22}$ in the He-Ne mixture) increases the stability of the system, since the asymmetry of the amplification curve weakens the coupling between the opposing waves. In addition, in a rotating ring laser, the region of instability of the opposing-wave regime increases with the speed of rotation, whereas in a gas ring laser there is no instability in the given approximation (as in [37]).

It is possible to obtain[38] two opposing traveling waves in a ring gas laser by solving Maxwell's equations in a slowly rotating coordinate system, using the procedure of [32]. The analysis is then continued in the usual manner: the same kinetic equations are analyzed, the polarizability of the medium is obtained in the third order of perturbation theory, the self-consistency equation is obtained for the amplitude and the phases, and the conditions for the stability of the opposing-wave regime are determined. The important difference[38] from the procedure of [36] is that the coupling between the waves via the mirrors is taken into account.

In this approximation, with account taken of the terms of second order in the ratio of the natural line width to the Doppler width, there appears a standing-wave instability region near the center of the amplification line. The limit of the instability region, in the case of a homogeneously broadened line,[39] is

$$|\nu_n - \nu_m|_0 = 2\sqrt{\frac{-D + \sqrt{D^2 - 4AC}}{2A}},$$

at $\nu_n = -\nu_m$; A, C and D are functions of the level widths.

For an inhomogeneously broadened line, the symmetrical arrangement of the opposing waves relative to the center of the Doppler contour is unstable;[39] the half width of the instability region is

$$\delta\nu = \frac{\gamma_{ab}^2}{ku}\sqrt{\frac{2}{S}},$$
$$S = \frac{\gamma_{ab}}{\gamma_a} + \frac{\gamma_{ab}}{\gamma_b} - \frac{\gamma_{ab}\gamma_\delta}{\gamma_a\gamma_b},$$

where $\gamma_\delta$ is due to the spontaneous solution from the upper working level to the lower working level.

Thus, by taking into account the modulation of the population inversion at the beat frequency, obtained in third order of perturbation theory,[43-46] we find that the stability conditions of the two-wave regime are different in a gas ring laser than in a solid-state laser, these conditions being different for opposing traveling waves and for waves traveling in the same direction. The ratio of the traveling-wave amplitudes varies with the pumping.

When account is taken of the coupling between the waves, due to the reflection from the mirror and the temporal modulation of the population inversion, a regime may set in wherein waves with different amplitudes, traveling in opposite directions, become stable.[42]

In fifth order of perturbation theory, with allowance of terms of second order in the oscillation intensity, the

instability region decreases with increasing amplitude in the case of a laser at rest.[40] Since the laser has in the general case different values of resonator Q for the opposite directions, the two-wave regime is impossible in the region whose upper limit can greatly exceed the limit of the instability region.[40] Using the methods of [41], it can be shown that the widths of the stability region and of the region in which the two-wave regime is impossible increase with increasing pressure. The two-wave regime in a ring laser becomes possible in the entire range of detuning in which the self-excitation conditions are satisfied, provided the $Ne^{22}$ admixture is of the order of several percent.[40] This follows from the expression for the critical concentration of the impurity isotope, $N_2$

$$N_2 \geqslant \exp\left\{\frac{\mu_2^2}{2(ku)^2}\right\}\left[\frac{\gamma^2}{(ku)^2}+\frac{2|\delta|}{\eta_0}-\frac{3}{2}\theta_1\eta_0\right],$$

where

$$\mu_2 = \nu-\nu_{02}, \quad \theta_1 = \frac{2\gamma^2}{3\gamma_{ab}}\left(\frac{\gamma_{ab}}{\gamma_a+2\gamma_{ab}}+\frac{\gamma_{ab}}{\gamma_b+2\gamma_{ab}}\right),$$

$\eta_0$ is the excess of the pump level over threshold.

The Lamb procedure,[35] of course, is not the only one in the analysis of a gas ring laser. It is possible, as usual, to consider Maxwell's equations in a rotating coordinate system (analyzing the potentials $A(\mathbf{r}, t)$ and $\varphi(\mathbf{r}, t)$ in lieu of the field intensity), obtain the conditions for the self-consistent field and the equations for the amplitude and the phases, and calculate the polarizability of the active medium on the basis of the Schrödinger equation written out in the occupation-number space.[47,48]

In the case of a ring laser without an active medium, it was not necessary to ascertain from which mirror the output signal is to be picked off. For a ring laser this is important.[49] In a linear laser, the mirror surfaces determine uniquely the spatial distribution of the antinodes and nodes of the standing wave. In a (stationary) ring laser, the opposing traveling waves also form a standing wave, but the positions of the antinodes and nodes become indeterminate. The question becomes particularly interesting in a multimode regime. Rotation of the ring laser leads to a splitting of the frequencies, which can be regarded as a slow shift of the standing-wave pattern. On a photoreceiver this is registered as modulation of a constant signal at the beat frequency. The following reasoning can be employed:[49] If we write the expression for the field intensities, then the condition that the intensity change in the active medium be minimal leads to a connection between the phases of the neighboring modes. They differ by $\pi$. In a multimode regime this leads to a difference between the amplitudes of the beats obtained past mirrors that have different distances from the distance tube. The experimental results obtained for a ring resonator of triangular form, one of the legs of which contained an active medium (He-Ne mixture, $\lambda$ = 6328 Å), agree with the expected values. The inequality of the neighboring-mode amplitudes makes an additional contribution to the difference between the beat amplitudes.

The beat amplitudes differ also in the case of two discharge tubes, and with increasing number of modes the amplitude difference increases more sharply than in the case of a single discharge tube. The unequal distances between the tubes and the common mirror leads to an additional phase shift between the neighboring modes, and this in final analysis changes the ratio of the beat amplitudes.

The opinion that a change in the resonator dimensions influences both opposing waves in identical fashion is rejected in [49]. It is shown that the beat frequency is modulated by the frequency (phase) of the change in the resonator dimensions, leading to different output signals from different mirrors.

## 4. EXPERIMENTAL INVESTIGATION OF THE COMPETITION OF THE OPPOSING WAVES IN A RING LASER

Experimental investigations were made of the interaction between the traveling waves in a ring laser. In [50] they used a triangular resonator (one flat mirror, two spherical mirrors with R = 4 m, each side of the equilateral triangle was 121 cm), and a discharge tube with He-Ne mixture ($\lambda$ = 6328 Å) was placed in one of the legs of the resonator. One of the spherical mirrors had a transmission coefficient almost 20 times larger (T = 3.7%) than the two others. This mirror was backed by one more mirror, as a result of which the intensity of the beam traveling in the clockwise direction was 5–7 times larger than that of the opposing beam. If the return mirror was covered in the one-mode regime, then the coupling decreased, the number of modes increased to three, and the total output power dropped to almost one-half at the same pump power. The decrease of the coupling was obtained not only by increasing the transmission of the return mirror, but also by decreasing the transmission of the resonator in front of the return mirror.[51] A similar effect was attained by increasing the transmissions of the remaining mirrors of the resonator.

The experiment confirmed the instability, noted in [39], of the regime in which waves with frequencies that are symmetrical relative to the center of the inhomogeneously broadened line travel opposite to each other. The ring laser consisted of a resonator with two spherical mirrors (R = 1.8 m) and operating on the principle of refraction of a prism.[52] The laser operated at the wavelength $\lambda$ = 6328 Å and the $Ne^{20}$ isotope (99.4%) was used in the He-Ne mixture. The scanning system changed the length of the resonator; the change of power of the opposing beams was measured with two photoreceivers and was compared on a two-beam oscilloscope. With the saturation regime attained (but in the case of one mode in each of the opposing waves), suppression of one of the opposing waves was observed when the resonator frequency passed through the center of the Doppler contour. When the multimode regime set in, all the waves of one direction were suppressed when the condition of symmetrical arrangement relative to the center of the Doppler contour was satisfied. The stability of the two-wave regime was investigated experimentally very thoroughly in [53].

Besides the investigations of the gas ring laser, theoretical and experimental studies are being made of solid-state ring lasers. Most investigations are devoted to the traveling-wave regime.[54-60] In particular, the question

of obtaining the traveling-wave regime in a ring laser with an external additional mirror is theoretically considered in [56]. The calculation is based on the methods of long-line theory, and is valid for a ring resonator with any active medium.

In many cases, stabilization of the frequency of the gas ring laser may be necessary to increase the experimental accuracy. Methods for frequency stabilization of a linear gas laser[61-63] are fully applicable in this case, too. One must not forget that the frequency characteristics of the gas laser become worse as a result of instability in the discharge.[64,65] Persistent attention must therefore be paid to the methods of eliminating noise from a plasma (mixed pumping[66] and others).

## 5. FREQUENCY LOCKING IN A LASER WITH A RING RESONATOR

In the case when the frequencies of the self-oscillating system and the external force acting on it are close, three operating modes are possible:

1) periodic mode;

2) quasiperiodic mode with oscillations close to sinusoidal, whose amplitude and phase vary periodically (slowly);

3) beat mode (see, for example [67]).

These cases are frequently encountered in radio engineering, so that these modes have been analyzed in detail for vacuum-tube circuits. We shall stop to discuss the first of them in somewhat greater detail. It was first analyzed by the authors of [68,69].

An analysis of the regenerative amplifier circuit (Fig. 11) has revealed the following phenomenon.[69] When the generator frequency differs greatly from the signal frequency of the external emf $E_{ext}$, modulation takes place and is determined by the difference between $\nu_0$ and $\nu_S$. With increasing detuning, the generator frequency is pulled in by the external signal and at a certain sufficiently small difference $\Delta\nu = \nu_0 - \nu_S$ the beats disappear and only $\nu_S$ remains. This is called frequency locking or forced synchronization. The synchronization band width is

$$\frac{\Delta\nu}{\nu} \approx \frac{E_{ext}}{E_0}, \tag{5.1}$$

and the phase varies by $2\pi$ within the synchronization band.[69]

The phenomenon of frequency locking was investigated in detail for vacuum-tube circuits.[70,78] It is adequately treated in monographs and text books (see, for example, [79-82]). It should be noted that this phenomenon can take place also in the case of combination interactions such as resonance of the second kind,[87] etc. This investigation procedure was subsequently applied to the case of mutual synchronization of two generators.[83-86]

The oscillation-theory methods used to analyze forced synchronization of vacuum tube generators can be used in principle also for self-oscillating systems of any type.

The phenomenon of frequency locking is encountered already in a linear laser.[35] In the normal three-mode regime, when the distance between the beat frequencies $\nu_2 - \nu_1$ and $\nu_3 - \nu_2$ become sufficiently small, a jump in the beat frequency takes place. The smallest distance that can be maintained between the beat frequencies before they are locked is

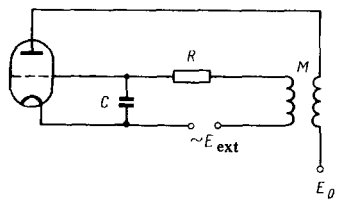


FIG. 11. Diagram of regenerative vacuum tube amplifier [69]. $E_0$ – supply-source voltage, $E_{ext}$ – amplitude of external signal.

$$\frac{\Delta\nu}{\nu} = \frac{1}{8Q}\frac{\bar{N}+2N_2}{\bar{N}_T}\left(\frac{pE_2}{\hbar\Delta}\right)^2, \tag{5.2}$$

where Q is the quality factor of the resonator, $\bar{N}$ the density of the excited atoms averaged over the resonator volume, $N_2$ the population of the upper working level, $\bar{N}_T$ the threshold value of the excitation at $\nu_1 = \nu_0$, p the dipole moment, $E_2$ the amplitude of the field with frequency $\nu_2$, and $\hbar$ Planck's constant.

The effect of frequency locking in a ring laser was first considered from the point of view of the action of an external force on the generator (and not mutual synchronization).[88] The case considered was that when the external action has a small amplitude. It was assumed that there is only one traveling wave in a triangular resonator (one leg with an active element).

From the boundary conditions for the electric field components it is possible to obtain the self-oscillation frequency in the case when there is no external signal. The appearance of the external signal leads to new boundary conditions. The self-oscillation frequency coincides with the frequency of the external signal if they differ by an amount smaller than a definite value $\epsilon$. The conditions for the maximum of $\epsilon$ give the locking band

$$\frac{\delta\nu}{\nu} = \frac{\lambda}{\pi L}\frac{ET}{U_0}, \tag{5.3}$$

where L is the perimeter of the ring resonator, E the external field, $U_0$ the amplitude of the self-oscillations, T the transmission of the mirror through which the external action is applied.

Forced synchronization in a laser with a ring resonator can be analyzed in greater detail by taking into account the mutual synchronization of the opposing waves.[89] Assuming the interaction to be sufficiently small, we can write an equation for the field

$$\ddot{E}_1 + \frac{\nu}{Q}\dot{E}_1 + \nu_1^2 E_1 = -4\pi\ddot{P}_1, \tag{5.4}$$

where

$$P_1 = \varkappa(E_1 + \bar{m}_1 E_2),$$
$$\bar{m}_1 = m_1 \exp(i\nu_1).$$

A similar equation holds for the opposing wave $E_2$. Putting

$$E_1 = e_1 E_0 \exp[i(\nu t + \varphi)],$$
$$E_2 = e_2 E_0 \exp[i(\nu t + \psi)], \tag{5.5}$$

where $e_i$ is the alternating part of the amplitude, and using the approximation of slowly varying phases and amplitudes, we can obtain equations for the latter.

In the synchronization regime we have

$$\frac{d(\varphi-\psi)}{dt}=0. \tag{5.6}$$

We put $\Phi = \varphi - \psi$. The condition for the stability of the synchronous regime is

$$\frac{d\left(\frac{\Delta\nu}{\nu}\right)}{d\Phi}\geqslant 0. \tag{5.7}$$

The equality in (5.7) yields the synchronization band

1) $\frac{\delta\nu}{\nu}=\frac{\gamma}{2k}\frac{\sqrt{4\beta^2+\mu^2}}{\mu}m$ if $m_1=m$, $m_2=0$;

2) $\frac{\delta\nu}{\nu}=Cm\left(\frac{3}{4}+\frac{1}{4}\sqrt{1+\frac{32D^2m^2}{C^2}}\right)\left(1-\frac{C^2}{32D^2m^2}+\frac{C^2}{32D^2m^2}\sqrt{1+\frac{32D^2m^2}{C^2}}\right)^{1/2}$

if $m_1 = m_2 = m$.

For $C \neq 0$ and $Dm \ll C$ we have

$$\frac{\delta\nu}{\nu}=Cm;$$

for $C \ll Dm$

$$\frac{\delta\nu}{\nu}=Dm^2.$$

We put $m_2 = m_1(1 + M)$; this yields

3) $\begin{cases}\frac{\delta\nu}{\nu}\approx\frac{\gamma m_1}{k}\left(\frac{2\beta}{\mu}\cos\chi+\sin\chi\right)(1+M) \text{ for } M\ll 1;\\ \frac{\delta\nu}{\nu}\approx\frac{\gamma m_1}{2k}\left(\frac{4\beta^2}{\mu^2}+1\right)^{1/2}M \text{ for } M\gg 1.\end{cases}$

The equation[47]

$$(\varphi_x-\Omega C_x)\alpha_x=-\mathrm{Re}\,(j_x+P_x)$$

(where $C_X = (1/4\pi C^2)\,\mathrm{Im}\int R_X[A_X\times[\nabla\times A_X]]dv\,dk$ is the wave amplitude), which describes the phases of the waves generated by the laser, can be reduced to the following system of equations for the opposing waves

$$\dot{y}_x=(\Omega C_x)-\frac{\omega_x}{2Q_x}-\mathrm{Re}\,\sigma_{-x,-x}-\frac{\alpha_x}{\alpha_{-x}}\mathrm{Re}\,\{(i-1)\eta_{-x,x}\exp(i\psi_{x,-x})\},$$
$$\dot{y}_{-x}=-(\Omega C_x)-\frac{\omega_x}{2Q_{-x}}-\mathrm{Re}\,\sigma_{-x,x}-\frac{\alpha_x}{\alpha_{-x}}\mathrm{Re}\,\{(i-1)\eta_{-x,x}\exp(i\psi_{-x,x})\},$$

where $\sigma_{X,X}$ is a characteristic of the frequency pulling (via scattering).

It follows from these equations that at a rotation velocity $\Omega \leq \Omega_3$ there will be no beats between the opposing waves. The width of the locking band is

$$\Omega_3=\frac{1}{C_x}|\eta|\sqrt{(1+\rho)^2+L_x^2}, \tag{5.8}$$

where $\eta$ is the summary coupling coefficient, and $\rho$ and $L_X$ take into account the Q of the resonator and the detuning, respectively. The forced synchronization band is proportional to the feedback echo coefficient.[47] The dependence of this band on the resonator Q and on the generation-frequency detuning relative to the Doppler contour has a minimum.

Analyzing the conditions for the stability and existence of a two-wave regime, we can find that in a definite region the beat frequency is a double-valued function of the generation frequency $\nu$.[47] The choice of the branch corresponding to the real course of the curve depends on the prior history (Fig. 12). This hysteresis phenomenon is due to the change of the refractive indices for the opposing waves under the influence of the laser radiation. The increase of the coupling between the wave and the decrease of the detuning leads to a broadening of the hysteresis band.

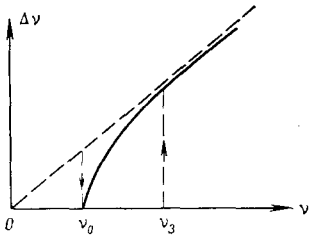


FIG. 12. Hysteresis of the dependence of the beat frequency $\Delta\nu$ on the generation frequency $\nu$ [47]. $\nu_0$ –lower locking frequency. $\nu_3$ – upper locking frequency.

An analysis of the intensity of the opposing beams yields a linear dependence of the intensity difference between the opposing beams on the angular velocity of rotation inside the frequency locking band.[47]

This dependence can be used to measure the angular velocity of rotation inside the locking band. In addition, it is possible to measure the angular velocity in the locking band by determining the phase difference of the opposing waves.[90] The connection between the angular velocity of the ring laser and the phase difference $\varphi$ is determined from the system of wave equations obtained with allowance for the back scattering from the mirrors and the inhomogeneities of the medium. Assuming that the laser generation frequency is sufficiently remote from the center of the Doppler line, we obtain[90]

$$\nu_1-\nu_2=\frac{\nu}{Q}\varepsilon\sin(\varphi-\varphi_0), \tag{5.9}$$

where

$$(2\varepsilon)^2=\varepsilon_1^2+\varepsilon_2^2+2\varepsilon_1\varepsilon_2\cos(\Delta_1-\Delta_2),$$
$$\varphi_0=\frac{\Delta_1+\Delta_2}{2}+\mathrm{arctg}\left\{\left[\frac{\varepsilon_1-\varepsilon_2}{\varepsilon_1+\varepsilon_2}\right]\mathrm{tg}\left(\frac{\Delta_1-\Delta_2}{2}\right)\right\}.$$

After experimentally determining $\epsilon$ and $\varphi_0$, the finding of the rotational velocity in accordance with (2.3) reduces to a measurement of $\varphi$ with the aid of an "optical phase meter."[90] The proposed "phase method" of measuring the velocity of rotation inside the locking band supplements the beat method used outside the locking band.

We can continue the list of papers devoted to an analysis of the locking conditions (see, for example [91,92]). It is still difficult, however, to use the results of these papers for the solution of applied problems.

An experimental study was also made of forced synchronization in a laser with a triangular resonator.[89] The dependence of the beat frequency on the detuning is shown in Fig. 13. The dependence of the locking band on the coupling between the waves (Fig. 14) also turns out to be as expected. In the case of a large coupling

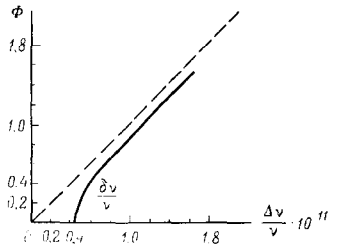


FIG. 13. Dependence of the beat frequency on the detuning [89]. $\Phi$–phase difference of opposing waves, $\Delta\nu/\nu$–relative beat frequency, $\delta\nu/\nu$–relative locking band.

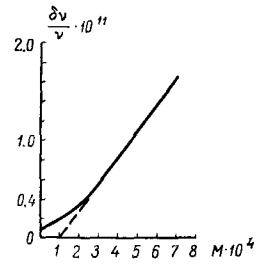


FIG. 14. Dependence of the locking band $\delta\nu$ on the coupling M between waves [89].

coefficient (which is regulated by means of an external mirror), the frequency locking disappears (this is also observed in radio engineering). The phase of the reflected wave also influences the size of the locking band. Unfortunately, the absolute values of $\delta\nu$ are not given in [89]. They can be found in [93-95], where a system with a square resonator configuration is described (0.5 meters on each side). Without special measures, the synchronization band was found to be 300-1000 Hz. By regulating the transparency of the mirrors, it is possible to reduce the locking band to 50 Hz.[95]

## 6. NONRECIPROCAL EFFECT AND POLARIZATION OF RADIATION IN A RING RESONATOR

Frequency splitting in a ring resonator is called a nonreciprocal effect.[96] This effect takes place not only when the ring resonator is rotated; for example, frequency splitting is observed when a post is placed in the path of a laser beam.[97] The experiment was performed in a square resonator (92 cm long) with generation at a wavelength $\lambda = 3.39\ \mu$. Beats of the order of 5 kHz were obtained when the point of a needle was inserted into the beam (approximately 1 mm away from the axis of the field). The effect is stronger when the needle is inserted near the Brewster window. It is assumed that the phenomenon is connected with the power-saturation effect. The object inserted into the laser beam changes the amplitudes of the opposing beams by different amounts, leading to a difference in the refractive index. There is no rigorous model of this effect, and no attempts were made to obtain the dependence of the frequency splitting on the system parameters. It may be that the approach used by the authors of [49] would be successful for the analysis of this phenomenon. It is possible that the phenomenon is due to different spatial distributions of the fields of the opposing waves.

Another method of splitting the frequency of a ring laser[97,98] is to place in the resonator a disc whose material has a refractive index n. Let the remainder of the resonator have a refractive index $n_0$. If the disc is rotated around an axis which does not lie in one plane with the laser beam, then the disc will have a velocity component $v_m$ along the optical path. Therefore the light crossing tht rotating disc will have a velocity

$$v_l = \frac{c}{n_0} \pm v_m \left(\frac{n^2-1}{n^2}\right)$$

(the coefficient of $v_m$ is called the Fresnel dragging coefficient). The refractive index of the disc is

$$n' = n \pm v_m \frac{n^2-1}{c}.$$

The wavelength generated by the laser is determined from the relation

$$N\lambda = (L-l)n_0 - ln' = Ln_0 - l(n-n_0) \pm lv_m \frac{n^2-1}{c},$$

where N is an integer. From this, on the basis of expression (2.8), the frequency splitting is given by the formula

$$\Delta\nu = 2lv_m \frac{n^2-1}{L\lambda}. \qquad (6.1)$$

By placing in the ring resonator a quartz disc at the Brewster angle, it is possible to observe beats at frequencies 1-20 kHz for an effective path of 17 mm in the quartz and for a longitudinal velocity, $v_m$ = 125-2500 mm/sec. The experimental points agree well with the calculated ones.[89] The nonreciprocal element, as noted in [89], may be not only a solid, but also a moving gas or liquid. For example, it is possible to blow air through a tube placed in one of the arms of the ring laser.[49] At low rotational velocities, it is necessary to take into account the splitting due to the earth's rotation.[4]

Another possible nonreciprocal element is a Faraday cell with polaroids:[2,53,99,100] a Faraday cell can be used not only in the main resonator, where they hinder the operation of the laser, but also in an external auxiliary resonator.[101,102]

Upon reflection from a dielectric surface, the plane of polarization is rotated through a certain angle A, which can be readily found with the aid of the Fresnel formula relating the electric field amplitudes E and R of the incident and reflected waves (see, for example, [7]):

$$R_p = E_p \frac{\operatorname{tg}(\alpha-\beta)}{\operatorname{tg}(\alpha+\beta)}$$

(p-polarization, the electric vector is in the plane of incidence),

$$R_s = -E_s \frac{\sin(\alpha-\beta)}{\sin(\alpha+\beta)}$$

(s-polarization), where $\alpha$ is the angle of incidence and $\beta$ the angle of refraction. Hence

$$\left.\begin{aligned} &\operatorname{tg} A_1 = \frac{E_p}{R_p}, \quad \operatorname{tg} A_2 = \frac{E_s}{R_s}, \quad A = A_1 - A_2, \\ &\frac{\operatorname{tg} A_1}{\operatorname{tg} A_2} = \frac{\cos(\alpha-\beta)}{\cos(\alpha+\beta)}. \end{aligned}\right\} \qquad (6.2)$$

The plane of polarization will not be rotated upon reflection from the dielectric in three cases: a) normal incidence, b) when the planes of polarization and incidence coincide, c) when the planes of polarization at incidence are orthogonal.

The first case is realized in a linear laser, so that operation with Brewster windows is possible for any position of the window planes.

If we consider the ring laser from this point of view, we are left with two other cases, of which the s-polarization is the better for the following reasons: First, the system is less sensitive to detuning, since A varies much more slowly in the vicinity of $\pi/2$ than in the vicinity of zero, given the same change of tan $A_i$. Second, automatic adjustment of the plane of polarization takes place in the vicinity of $A_i = \pi/2$ upon reflection from the mirror, whereas the opposite takes place in the vicinity of $A_i = 0$. Unfortunately, these two positions are of no practical use in a ring laser, for in this case the plane of the polarization of the radiation is determined by the resonator. Therefore external factors,

for example the rotation of a discharge tube with Brewster windows, will not lead to a simultaneous change of both the radiation power and of the radiation polarization plane.[103]

Thus, the generation that is possible in a ring laser can have only two directions of the electric field vector E: E either lies in the plane of the resonator or is perpendicular to it. It is seen from (6.2) that for p-polarization the phases of E and R coincide only when the incidence angles are larger than the Brewster angle. This imposes one more limitation on the p-polarization (in [103] it is introduced erroneously as s-polarization). In practice (triangular and quadrangular resonators) no p-polarization is encountered (the incidence angles are smaller than the Brewster angle).

The most complete analysis of the polarization of laser radiation was made in [104], where the Poincare-sphere method was extensively used. This method was also used by the authors of [105] to investigate a ring laser with an isotropic element.

## 7. OPTIMAL PARAMETERS OF A RING LASER

The laser radiation power is determined primarily by the population inversion ΔN. In order to make the latter maximal, the parameters of the active medium are chosen to be optimal: a definite electron concentration $n_e$ is produced in the plasma, as well as a definite electron temperature $T_e$. In practice this reduces to the proper choice of the discharge power supply and of the gas parameters (or gas mixture).

The fundamental-mode field distribution over the resonator cross section E(x, y) has a Gaussian form.[8-10] If spherical mirrors are used in the resonator, then the longitudinal field distribution of the resonator is likewise not constant. In the case of a "plane–sphere" resonator, the resonator field distribution is a curve of the Gaussian type, the maximum of which decreases and the width increases on going from the flat mirror to the spherical one. The field distribution on the mirrors of a semi-confocal resonator is shown in Fig. 15.

The population inversion in the active laser medium is also unevenly distributed. In the gas discharge, the concentration of the excited atoms in an infinite cylinder should satisfy the equation[106-108]

$$D_a\left(\frac{d^2N}{dr^2}+\frac{1}{r}\frac{dN}{dr}\right)+\alpha_a n_a q_e=\beta_a N q_e+\gamma_a N, \qquad (7.1)$$

where $D_a$ is the diffusion coefficient; $n_a$ and N—concentrations of the normal and excited atoms, $q_e = n_e(r)/n_e(0)$, $n_e(0)$—concentration of the electrons on the cylinder axis, $n_e(r)$—radial distribution of the electron concentration; $\alpha_a$—probability of collisions of the first kind between the atoms and electrons on the cylinder axis; $\gamma_a$—probability of atomic collisions of the second kind (on the axis); $\beta_a$—probability of collisions of the second kind between atoms and electrons.

The boundary conditions are

$$\left.\frac{dN}{dr}\right|_{r=0}=0, \quad N|_{r=a}=0.$$

Two limiting cases are possible:

1) $\gamma_a \gg \beta_a$; then (7.1) has a solution

$$N(r)=N(0)\,J_0\left(\mu_1\frac{r}{a}\right),$$

where

$$N(0)=\frac{n_a\alpha_a}{\gamma_a+\frac{\mu_1^2 D_a}{a^2}};$$

$J_0(\mu_1 r/a)$ is a Bessel function of zero order, $\mu_1$ is the first root of this function, and a is the radius of the cylinder.

2) $\beta_a \gg \gamma_a$; the solution of (7.1) is

$$N=N_{B_a}\left[1-\frac{I_0\left(\sqrt{B_a}\frac{r}{a}\right)}{I_0\left(\sqrt{B_a}\right)}\right],$$

where $N_M$ is the concentration of the excited atoms in the case of a Maxwellian energy distribution: $B_a = \beta_a a^2/D_a$; $I_a(\sqrt{B_a})$ is a Bessel function of imaginary argument. At small $B_a$ (smaller than 10) both solutions are close in form.

If we wish to consider the population inversion ΔN, then we must take into account not one excited level, as in (7.1), but at least two levels. For example, for an He-Ne laser it is necessary to solve the equations for the $3s_2$ and $2p_4$ levels of neon (we refer here to the excitation line with $\lambda = 0.6328\ \mu$). In addition, it is necessary to take into account the 1s level of neon[125] and the d levels of neon.[109,110] In the first approximation we can simplify the problem for the He-Ne mixture and consider separately only two working levels. For excited helium atoms $2^1S$) we can write an expression similar to (7.1)[111]

$$D_a\left(\frac{d^2N_{He}}{dr^2}+\frac{1}{r}\frac{dN_{He}}{dr}\right)+\alpha n_{He}n_e=\beta N_{He}n_e+\gamma N_{He}N_{Ne}, \qquad (7.2)$$

where $\alpha n_e n_{He}$ is the number of helium atoms excited by electron impact in the $2^1S$ state, $\beta n_e N_{He}$ is the number of metastable helium atoms destroyed by electron impact, $\gamma N_{He} N_{ne}$ is the number of neon atoms excited by helium atoms in the state $2^1S$, and $n_e = n_e(0) J_0(\mu_1 r/a)$.[112] Assuming that the number $N(2p_4)$ of neon atoms excited in the state $2p_4$ is proportional to $n_e$, and that the number $N(3s_2)$ of neon atoms excited in the state $3s_2$ is proportional to $N_{He}$, we can assume[111] that the inversion of the populations in this case is $\Delta N(n/a)$

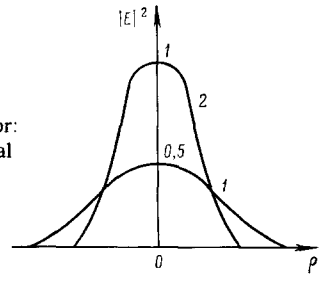


FIG. 15. Radial distribution of the field in a semiconfocal resonator: 1—field distribution on the spherical mirror, 2—on the flat mirror.

$= \text{const} \cdot J_0(\mu_1 r/a)$. The experimentally measured quantity was not $\Delta N(r/a)$ but the amplification coefficient of the He-Ne mixture for the radiation with $\lambda = 0.6328\ \mu$, which has the same radial distribution as $\Delta N(r/a)$, and good agreement was obtained.[111]

The radial distribution of the population inversion in the He-Ne discharge changes with the discharge current: it first increases in the same manner as the current becomes smeared out, and finally saturation produces a dip on the axis. The distribution varies with pressure (there is an optimal pressure at which ΔN on

the axis is maximal), and absorption of the radiation is observed starting with a certain pressure; the distribution also varies with the ratio of the mixture components (it becomes sharper with increasing fraction of helium); there exists an optimal component ratio at which $\Delta N$ is maximal on the axis[113-115] (Fig. 16).

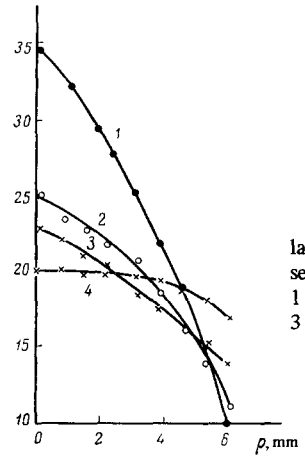


FIG. 16. Distribution of the population inversion (gain) over the cross section $\rho$ of the discharge tube [114, 115]. 1 – $P_{He}/P_{Ne}$ = 7 : 1; 2 – 5 : 1; 3 – 3 : 1; 4 – 1 : 1; P = 0.8 torr.

Thus, the resonator field and the population inversion have uneven distributions in the active medium. Apparently, the laser radiation power is determined not by the absolute value of $\Delta N$ in the active medium, but only by the part that is in the region of the resonator field distribution and interacts effectively with the field.[115] In other words, the laser radiation power is determined by the region where the distributions indicated above overlap.

Inasmuch as the distribution of the population inversion changes with the pump and with the mixture parameters, it is possible to use the latter to regulate the "overlap region," meaning also the output power of the laser. In turn this means that the parameters of the He-Ne mixture are optimal, depending on the type of the resonator used in the He-Ne laser.[115] There is a widely help opinion that for a He-Ne laser (with $\lambda = 0.6328\ \mu$ and $\lambda = 3.39\ \mu$), the optimal component ratio is $P_{He}/P_{Ne}$ = 5:1, and the pressure is determined from the relation pD = 2.9–3.6 torr-mm.[116] The results of [116] were confirmed in some investigations (see, for example, [117]). The point is that these measurements were carried out in a confocal (semi-confocal) resonator, and the length of the discharge gap was approximately equal to the resonator length. If a discharge tube much shorter than the resonator is placed in a semiconfocal resonator (Fig. 17a), then the optimal parameters of the He-Ne mixture are determined by the location of the tube in the resonator.[118] The resonator field at the spherical mirror is more smeared out than at the flat mirror. Assuming that the laser radiation power is maximal when the resonator field and the population inversion have similar distributions, we can expect (on the basis of the results of [114-115]) that by placing the tube near the spherical mirror it is possible to obtain one optimal mixture-component ratio $n_1 = P_{He}/P_{Ne}$, and by placing it near the flat mirror it is possible to obtain another optimal component ratio $n_2$, with $n_2 > n_1$.

Indeed, in [118], a tube of length $l$ = 20 cm, was placed in a resonator of length L = 1 m (the tube diameter, 3 mm, was much larger than the "wave spot" on the spherical mirror of the resonator for the fundamental mode), and the result was $n_1$ = 3.5:1 and $n_2$ = 6.5:1 ($\lambda = 0.6328\ \mu$). In the case of a non-confocal resonator, the deviation of the maximum value of $P_{He}/P_{Ne}$ from 5:1 will be observed for tubes of any length. In accordance with the foregoing considerations, the optimal n in a "plane–sphere" resonator at $L \approx l$ will be larger than 5:1 if $R < 2L$ (R—radius of curvature of the mirror). When $R > 2L$, the optimal n becomes smaller than 5:1. Thus, in [119], in a resonator with $L \approx 1$ m ($l \approx L$, 2 diameter 6 mm), one spherical mirror was used with R = 1.5 m. An optimal ratio $P_{He}/P_{Ne}$ = 9:1 is obtained at a pressure $p \approx 2$ torr ($\lambda = 0.6328\ \mu$).

In a ring He-Ne laser, in the presence of spherical mirrors, it is also necessary to take into account the phenomenon described above. By virtue of the fact that the resonator field distribution will be different in the different arms, one should expect changes in the optimal parameters for tubes placed in arms with different field distributions. The reasoning advanced for the res-

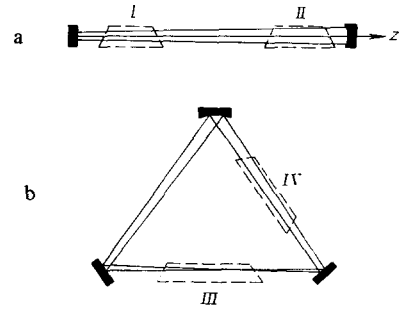


FIG. 17. a) Semiconfocal resonator with short tube; b) ring resonator.

onator of Fig. 17a can be used also for the resonator of Fig. 17b. The optimal mixture component ratio n is expected to be larger than 5:1 in arm III and smaller than 5:1 in arm IV. For a ring laser with resonator shown in Fig. 17b (arm 120 cm, tube with $l$ = 1 m, D = 6 mm, R = 3 m), an optimal component ratio ($\lambda = 0.6328\ \mu$) of 3:1 was obtained in arm IV and 6:1 in arm III.[120] Using spherical mirrors with R larger than the perimeter of the triangle, a smoothing of the differences between the arms was observed in [120], this being apparently connected with the change of the resonator field configuration.

So far we have considered only the possibility of changing the radial distribution of the population inversion. Account should also be taken of the longitudinal distribution of the population inversion. In a cylindrical tube, it is practically homogeneous.

In a tube with a conical cross section[121] it becomes inhomogeneous, and the total gain increases. Indeed, the gain per unit length of the discharge gap on the axis of a cylindrical tube of an He-Ne laser is $G = G_0 k_0$,[122] where $G_0$ is the function of the state of the active medium, determined by the discharge current, by the pressure, and by the ratio of the mixture component, and $k_0$

is determined by the tube geometry ($k_0 \approx 1/a$ for an He-Ne laser). Being interested only in the dependence of the geometry of the cross section, we can make the remaining conditions identical. We therefore seek the geometrical part of the gain coefficient for a cylindrical tube, in the form

$$k = \frac{1}{S} \int k_0 f(S)\, dV, \qquad (7.3)$$

where V is the volume of the tube, and S is the area of the cross section. For a cylindrical tube, assuming $f(S) = J_0(\mu_1 r/a)$, we have $k = 0.43\, l/a$. For a tube with a quadratic cross section of the same area, $k = 0.45\, l/a$. Using (7.3) for the tube proposed in [121], we get

$$k = \frac{2\pi}{S_{cp}} \int_0^l \int_0^{r_0} \frac{1}{r_0} J_0\left(\mu_1 \frac{r}{r_0}\right) r\, dr\, dz, \qquad (7.4)$$

where

$$r_0 = b + \frac{a-b}{l} z,$$

$$S_{cp} = \frac{1}{l} \int_0^l \pi r_0^2\, dz = \frac{\pi}{3}(a^2 + ab + b^2),$$

a and b are the radii of the ends of the conical tube. By placing the conical-cross-section tube in a confocal ring laser (Fig. 18), we obtain in accordance with (7.4), $k = 0.475\, l/a$ for $a/b = 1.2$ (the spots on the mirrors of this resonator differ by approximately the same factor). A still greater gain can be obtained by using parabolic generatrices in a conical tube. Consequently, the use of a tube with conical cross section in an He-Ne ring laser is more advantageous than the use of a cylindrical tube. Further optimization of the ring laser can be obtained by placing tubes of different diameters[123] and different cross sections in the different arms of the resonator.

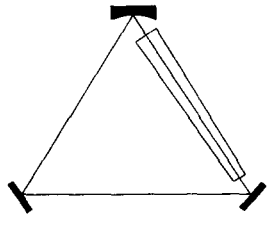

FIG. 18. Tube of conical cross section in a ring resonator.

Thus, the use of the distribution of the population inversion is one more source of increasing the power of gas lasers, including ring lasers. To increase the efficiency of utilization of this source, naturally, it is necessary to investigate exhaustively the plasma of the gas laser. This will make it possible, in particular, to obtain a more rigorous interpretation of the results of [111,113,114]. The probe and resonator plasma-parameter measurements performed to data,[124-127] and also theoretical studies of the problem (see, for example, [128]) do not make it possible to assume that the dependence of the radiation power on the plasma parameters has been completely determined. Individual attempts, using known data on the behavior of a plasma,[129,130] to predict the dependence of the He-Ne laser power on the discharge parameters (see, for example, [62,131]), make it possible to make only qualitative estimates. To solve the problem of the role of the plasma parameters in processes that take place in a gas laser it is therefore necessary to improve further the procedures for laser-plasma research.


[1] W. M. Maček and D. T. M. Davis, Appl. Phys. Lett. 2, 67 (1963).
[2] E. J. McCartney, Navigation 13, 260 (1966).
[3] P. J. Klass, Aviation Week and Space Techn. 85, 103 (1966).
[4] A. L. Shawlow, Sci. Amer. 209, 34 (1963).
[5] R. C. Langford, Sciences et Techn. de l'arm. 39, 399 (1965).
[6] L. D. Landau and E. M. Lifshitz, Teoriya Polya, Fizmatgiz, 1962 [Classical Theory of Fields, Addison-Wesley, 1965].
[7] A. Sommerfeld, Optics (Russ. Transl.), IL, 1953.
[8] A. G. Fox and T. Li, Bell Syst. Techn. J. 40, 453 (1961).
[9] G. D. Boyd and H. Kogelnik, Bell Syst. Techn. J. 41, 1347 (1962).
[10] G. D. Boyd and J. P. Gordon, Bell Syst. Techn. J. 40, 489 (1961).
[11] L. A. Vaĭnshteĭn, Zh. Eksp. Teor. Fiz. 44, 1050 (1963) [Sov. Phys.-JETP 17, 709 (1963)].
[12] V. S. Buldyrev and E. E. Fradkin, Opt. spektr. 17, 583 (1964).
[13] E. E. Fradkin, ibid. 20, 316 (1966).
[14] L. A. Vaĭshteĭn, Otrkytye rezonatory (Open Resonators), Sov. Radio, 1966.
[15] C. L. Tang, Appl. Optics 1, 768 (1962).
[16] P. Smith and T. Li, Proc. IEEE 53, 459 (1965).
[17] S. A. Collins, Appl. Optics 3, 1263 (1964).
[18] V. A. Kiselev, Zh. prikl. spektr. 4, 37 (1966).
[19] V. A. Kiselev, ibid. 4, 230 (1966).
[20] V. A. Kiselev, ibid. 5, 23 (1966).
[21] V. A. Kiselev, ibid. 6, 45 (1967).
[22] S. A. Collins and D. T. M. Davis, Appl. Optics 3, 1314 (1964).
[23] V. S. Buldyrev and M. M. Popov, Opt. spektr. 20, 905 (1966).
[24] M. M. Popov, Vestnik LGU 4, 42 (1967).
[25] M. G. Sagnac, Compt. Rend. 157, 708 (1913).
[26] M. G. Sagnac, J. Phys. 4, 5, 177 (1914).
[27] M. P. Langevin, Compt. Rend. 173, 831 (1921).
[28] A. H. Rosental, JOSA 52, 1143 (1962).
[29] I. P. Mazan'ko, Zh. prikl. spektr. 1, 153 (1964).
[30] E. O. Shulz-DuBois, IEEE-QE 2(8), 299 (1966).
[31] C. V. Heer, Bull. Amer. Phys. Soc. 6, 58 (1961).
[32] C. V. Heer, Phys. Rev. 134, A799 (1964).
[33] J. C. Slater, Microwave Electronics, Van Nostrand, 1950.
[34] A. M. Khromykh, Zh. Eksp. Teor. Fiz. 50, 281 (1966) [Sov. Phys.-JETP 23, 185 (1966)].
[35] W. E. Lamb, Phys. Rev. 134, A1429 (1964).
[36] F. Aronowitz, Phys. Rev. 139, A635 (1965).
[37] J. A. White, Phys. Rev. 137, A1651 (1965).
[38] B. L. Zhelnov, A. P. Kazantsev, and V. S. Smirnov, Zh. Eksp. Teor. Fiz. 50, 1291 (1966) [Sov. Phys.-JETP 23, 858 (1966)].
[39] S. G. Zeĭger and É. E. Fradkin, Opt. spektr. 21, 386 (1966).
[40] Yu. L. Klimontovich, P. S. Landa, and V. A. Larionsev, Zh. Eksp. Teor. Fiz. 52, 1616 (1967) [Sov. Phys.-

JETP 25, 1076 (1967)].
[41] S. G. Rautian and I. I. Sobel'man, Usp. Fiz. Nauk 90, 209 (1966) [Sov. Phys.-Usp. 9, 701 (1967)].
[42] B. L. Zhelnov and V. S. Smirnov, Opt. spektr. 23, 331 (1967).
[43] S. G. Zeĭger, Izv. vuzov (Radiofizika) 10, 1671 (1967)].
[44] S. G. Zeĭger, Dokl. Akad Nauk SSSR 177, 554 (1967) [Sov. Phys.-Dokl. 12, 1054 (1968)].
[45] S. G. Zeĭger, Zh. Tekh. Fiz. 38, 68 (1968) [Sov. Phys.-Tech. Phys. 13, 48 (1968)].
[46] S. G. Zeĭger, Candidate's dissertation (Leningrad State Univ., 1967).
[47] G. S. Kruglik, K teorii bieniĭ v kol'tsevom OKG (Theory of Beats in Ring Lasers), Minsk, 1967.
[48] G. S. Kruglik, Zh. Prikl. spektr. 7, 569 (1967).
[49] I. L. Bershteĭn and Yu. M. Zaĭtsev, Zh. Eksp. Teor. Fiz. 49, 953 (1965) [Sov. Phys.-JETP 22, 663 (1966)].
[50] S. N. Bagaev, V. S. Kuznetsov, et al., ZhETF Pis. Red. 1 (No. 4), 21 (1965) [JETP Lett. 1, 114 (1965)].
[51] E. M. Belenov, E. P. Markin et al., ibid. 3, 54 (1966) [3, 32 (1966)].
[52] V. N. Lisitsyn and B. I. Troshin, Opt. spektr. 22, 66 (1967).
[53] T. J. Hurchings et al., Phys. Rev. 152, 467 (1966).
[54] C. L. Tang et al., Phys. Rev. 136, 1A (1964).
[55] M. Hercher et al., J. Appl. Phys. 36, 3351 (1965).
[56] V. Yu. Petrun'kin et al., Radiotekhn. i élektron. 12, 467 (1966).
[57] A. M. Bonch-Bruevich, V. Yu. Petrun'kin, et al., Zh. prikl. spektra. 6, 540 (1967).
[58] A. M. Bonch-Bruevich, V. Yu. Petrun'kin, et al., Zh. Tekh. Fiz. 37, 2031 (1967) [Sov. Phys.-Tech. Phys. 12, 1495 (1968)].
[59] V. Yu. Petrun'kin et al., Abstracts of VTK LPI, Radio-electronics Series, Moscow, 1967.
[60] A. M. Bonch-Bruevich, V. Yu. Petrun'kin et al., Proc. Conf. on Quantum Electronics, Popov Institute, Moscow, 1967.
[61] A. D. White, IEEE-QE 1, 349 (1965).
[62] M. I. D'yakonov and S. A. Fridrikhov, Usp. Fiz. Nauk 90, 565 (1966) [Sov. Phys.-Usp. 9, 837 (1967)].
[63] A. B. Birnbaum, IRE Proc. 55, 308 (1967) (Russ. Transl.).
[64] A. V. Nedospasov, Usp. Fiz. Nauk 94, 439 (1968) [Sov. Phys.-Usp. 11, 174 (1968)].
[65] L. Pekarek, ibid. 94, 463 (1968) [11, 188 (1968)].
[66] S. A. Alyakishev, D. V. Gordeev, E. P. Ostapchenko, and L. M. Pyatkova, Radiotekh. i élektron. 12, 1769 (1967).
[67] Yu. B. Kobzarev, Zh. Tekh. Fiz. 5, 216 (1935).
[68] B. Van der Pol, Radio Revue 1, 701 (1920).
[69] H. G. Møller, Jahrb drahtlosen Telegr. u. Teleph. (Brl.) 19, 28 (1922).
[71] E. Appleton, Proc. Cambridge Phil. Soc. 21, 231 (1922).
[72] F. Ollendorf, Arch. Electrotech. 16, 280 (1926).
[73] B. Van der Pol, Phil. Mag., ser. 7, 3, 65 (1927).
[74] A. A. Andronov and A. A. Vitt, ZhPF 7, 3 (1930).
[75] G. Petrosyan, P. Ryazin, and K. Teodorchik, Zh. Tekh. Fiz. 3, 1051 (1933).
[76] P. Ryazin, ibid. 5, 38 (1935).
[77] E. Sekarskaya, ibid. 5, 253 (1935).
[78] Z. Jelonek, H. Techn. El. Ak. 46, 164 (1935).
[79] N. I. Krylov, Élektricheskie protsessy v nelineĭnykh élementakh radiopriemnikov (Electric Processes in Nonlinear Elements of Radio Receivers), M., 1949.
[80] K. F. Teodorchik, Avtokolebatel'nye sistemy (Self-oscillating Systems), Gostekhizdat, 1952.
[81] I. M. Kapchinskiĭ, Metody teorii kolebaniĭ v radiotekhnike (Methods of Oscillation Theory in Radio Engineering), Gostekhizdat, 1954.
[82] I. S. Gonorovskiĭ, Osnovy radiotekhniki (Principles of Radio Engineering), Svyaz'izdat, 1957.
[83] A. G. Maĭer, Tech. Phys. USSR 2, 465 (1935).
[84] V. I. Gaponov, Zh. Tekh. Fiz. 6, 801 (1936).
[85] K. F. Teodorchik, Radiotekhnika 1, 3 (1946).
[86] I. Esafov, Zh. Tekh. Fiz. 6, 803 (1947).
[87] L. I. Mandel'shtam and N. D. Papaleksi, ibid. 2, 775 (1932).
[88] I. L. Bershteĭn, Dokl. Akad. Nauk SSSR 163, 60 (1965) [Sov. Phys.-Dokl. 10, 607 (1966)].
[89] Yu. L. Klimontovich, V. N. Kuryatov, and P. S. Landa, Zh. Eksp. Teor. Fiz. 51, 3 (1966) [Sov. Phys.-JETP 24, 1 (1967)].
[90] N. N. Rozanov and G. I. Vinokurov, and O. B. Danilov, Opt. Spektrosk. 23, 624 (1967).
[91] F. Aronowitz,and R. J. Collins, Appl. Phys. Lett. 9, 55 (1966).
[92] C. L. Tang and J. A. Statz, J. Appl. Phys. 38, 323 (1967).
[93] V. S. Letokhov and E. P. Markin, Zh. Eksp. Teor. Fiz. 48, 770 (1965) [Sov. Phys.-JETP 21, 509 (1965)].
[94] N. G. Basov et al., Trudy, Phys. Inst. Acad. Sci. (Quantum Radiophysics) 31, 113 (1965).
[95] E. M. Belenov, E. P. Markin, et al., ZhETP Pis. Red. 3, 54 (1966) [JETP Lett. 3, 32 (1966)].
[96] P. K. Cheo and C. V. Heer, Appl. Optics 3, 788 (1964).
[97] W. M. Maček et al., J. Appl. Phys. 35, 2556 (1964).
[98] H. Yee, Sciences et Techn. de l'arm. 39, 443 (1965).
[99] N. D. Milovskii, Izv. vuzov (Radiofizika) 7, 1095 (1964).
[100] A. L. Mikaelyan et al., Radiotekhn. i élektron. 11, 12 (1966).
[101] R. S. Smith and L. S. Watkins, Proc. IEEE 53, 188 (1965).
[102] L. S. Watkins and R. S. Smith, Sciences et Techn. de l'arm. 39, 451 (1965).
[103] S. N. Bagaev, Yu. V. Troitskiĭ, and B. I. Troshin, Opt. Spektrosk. 21, 768 (1966).
[104] H. de Lang, Polarization Properties of Optical Resonators..., Eindhoven, Netherlands, 1966.
[105] B. I. Troshin and S. I. Bagaev, Opt. Spektrosk. 23, 781 (1967).
[106] V. A. Fabrikant, Zh. Eksp. Teor. Fiz. 8, 549 (1938).
[107] V. A. Fabrikant, Dokl. Akad. Nauk SSSR 19, 385 (1938).
[108] V. A. Fabrikant, Trudy VEI 41, 236 (1940).
[109] A. S. Khaĭkin, ZhETF Pis. Red. 3, 110 (1966) [JETP Lett. 3, 68 (1966)].
[110] A. S. Khaĭkin, Zh. Eksp. Teor. Fiz. 51, 38 (1966) [Sov. Phys.-JETP 24, 25 (1967)].
[111] C. Herziger, Zs. Phys. 189, 385 (1966).
[112] A. von Engel, Ionized Gases, Oxford, 1965.
[113] Yu. V. Troitskii and V. P. Chebotaev, Opt. Spektrosk. 20, 362 (1966).
[114] V. E. Privalov and S. A. Fridrikhov, Zh. prikl.

spektr. 9, 320 (1968).
[115] Yu. M. Golubev, V. E. Privalov, S. A. Fridrikhov, and V. A. Khodovoĭ, Zh. Tekh. Fiz. 38, 1097 (1968) [Sov. Phys.-Tech. Phys. 13, 833 (1968)].
[116] A. D. White and J. D. Rigden, Appl. Phys. Lett. 2, 211 (1962).
[117] A. F. Korolev, A. I. Odintsov, and V. N. Mitsai, Opt. Spektrosk. 19, 71 (1965).
[118] V. E. Privalov and V. A. Khodovoĭ, ibid. 25, 318 (1968).
[119] Yu. M. Golubev, V. E. Privalov, ibid. 22, 499 (1967).
[120] Yu. M. Golubev, V. E. Privalov, S. A. Fridrikhov, and V. A. Khodovoĭ, Zh. Tekh. Fiz. 38, 1990 (1968) [Sov. Phys.-Tech. Phys. 13, 1598 (1969)].
[121] B. P. Miretskiĭ, E. P. Ostapchenko, S. G. Sedov, and A. A. Fedotov, Abstracts of Papers at Scientific and Tech. Conf. on Quantum Electronics, Moscow, 1967.
[122] W. R. Bennett, Jr., Usp. Fiz. Nauk 81(1) 119 (1963).
[123] See [121], p. 6.
[124] A. E. Fotiadi and S. A. Fridrikhov, Zh. Tekh. Fiz. 37, 566 (1967) [Sov. Phys.-Tech. Phys. 12, 406 (1967)].
[125] L. F. Vellikok, A. E. Fotiadi, and S. A. Fridrikhov, ibid. 37, 1127 (1967) [12, 811 (1967)].
[126] I. M. Belousova, O. B. Danilov, and I. A. El'kina, ibid. 1681 (1967) [12, 1229 (1968)].
[127] I. M. Belousova, O. B. Danilov, I. A. El'kina, and V. M. Kiselev, Opt. Spektra. 24, 779 (1968)].
[128] A. I. Maksimov, Opt. Spektr. 22, 188 (1967).
[129] V. E. Golant, M. V. Krivosheev, and V. E. Privalov, Zh. Tekh. Fiz. 34, 953 (1964) [Sov. Phys.-Tech. Phys. 9, 737 (1964)].
[130] E. F. Labuda and E. J. Gordon, J. Appl. Phys. 35, 1647 (1964).
[131] V. E. Privalov and S. A. Fridrikhov, Zh. Tekh. Fiz. 38, 1607 (1968) [Sov. Phys.-Tech. Phys. 13, 1303 (1969)].

**Literature Added in Proof**

[132] E. M. Belenov and A. N. Oraevskiĭ, Dokl. Akad. Nauk SSSR 180, 56 (1968) [Sov. Phys.-Dokl. 13, 411 (1968)].
[133] E. M. Belenov and E. P. Markin, ZhETF Pis. Red. 7, 497 (1968) [JETP Lett. 7, 381 (1968)].
[134] S. G. Zeĭger and É. E. Fradkin, Izv. vuzov (Radiofizika) 11, 519 (1968).
[135] V. Yu. Petrun'kin, N. A. Esepkina, et al., Radiotekhn. i élektron. 12, 146 (1967).
[136] A. M. Bonch-Bruevich, V. Yu. Petrun'kin, et al., Zh. prikl. spektr. 6, 540 (1967)].
[137] P. S. Landa, E. G. Lariontsev, and G. A. Chernobrovkin, Radiotekh. i Elektron. 13, 2026 (1968).
[138] V. E. Privalov and S. A. Fridrikhov, Zh. Tekh. Fiz. 38, 2080 (1968) [Sov. Phys.-Tech. Phys. 13, 1667 (1969)].

Translated by J. G. Adashko